SIXTH FRAMEWORK PROGRAMME
FP6-2002-INCO-MPC-1

MEditerranean Development of Innovative Technologies for integrAted waTer managEment

Project no.PL 509112

MEDITATE

MEditerranean **D**evelopment of **I**nnovative **T**echnologies for integr**A**ted wa**T**er manag**E**ment

STREP

Thematic Priority :
INCO Mediterranean Countries, B1 « Environement integrated mangaement of limited water resources »

AUV for submarine karst springs
(WP3 - Final Repport)

Start date of project: 1st May 2004
Duration: 42 months

LIRMM, L. Lapierre, B. Jouvencel
Submission date = October 2007

Project co-funded by the European Commission within the Sixth Framework Programme (2002-2006)		
Dissemination Level		
PU	Public	
PP	Restricted to other programme participants (including the Commission Services)	
RE	Restricted to a group specified by the consortium (including the Commission Services)	
CO	Confidential, only for members of the consortium (including the Commission Services)	X

TABLE OF CONTENT

Goals of the WP3 package

The objective of the LIRMM partner in the WP3 package is to design, validate and test the use of an AUV (Autonomous Underwater Vehicle) in the study of underwater springs, in order to autonomously detect and acquire a sufficient amount of water measurements for quantifying the quality of the sweet water discharge. The work has been organized according to 8 different tasks :

a. **Task A.1**. **Define the pay-load of vehicle**.
   Selection of sensors (Conductivity Temperature Depth, loch, sonar, Doppler, GPS…).
   Determination of the best positioning of sensors according the desired precision of measurements.

b. **Task A.2**. **Performances of the AUV**.
   Determination of the capacity of the vehicle to follow pre-defined paths, and quantification of the error the vehicle tracking.
   Quantification the system autonomy (Energy).

c. **Task A.3**. **Protocol to define for scientist missions**:
   Specify the Man-Machine Interface that allows for deploying the AUV by scientists.

d. **Task A. 4. Development of vehicle and sensors integration**
   Development of the AUV, including the necessary sensor suite.

e. **Task A. 5**. **Study of fusion data method to build a 3D representation**
   Development of the necessary software suite in order to fuse the measurements in a comprehensive form.

f. **Task A. 6**. **Test of vehicle**
   Realization of the necessary validation tests in order to start the springs survey.

g. **Task A. 7**. **Submarine springs survey**
   Realization of the spring survey on different selected sites, and results presentation.

h. **Task A.8**. **Feasibility study**
   Concerning the use of the AUV in the Scope of the Meditate project.

Vehicles specifications, presentation and evolution

The LIRMM is equipped with 2 AUVs, named Taipan 2 and Taipan 300, which have been equipped and deployed in the scope of the Meditate Project, according to the specifications defined in the Deliverable 1: “AUV specifications”. The guidelines are summarized below :

Taipan 2

The AUV Taipan 2 has been developed by the laboratory LIRMM in collaboration with the French company Hytec. It is a torpedo-shape vehicle with a length of 1.7 meter, a diameter of 20 cm, and a weight of 60kg (figure 1 and 2). It is propelled with a back thruster and driven with 6 control surfaces (cf. fig. 3). The autonomy is approximately 4 hours with a 4 knots forward velocity. A complete navigation sensors suite has been integrated for odometric positioning during the immersion, with a GPS correction when surfacing. The vehicle is also equipped with scientific sensors, which allows for CTD sampling (conductivity, Temperature, Depth) and acoustic and video images acquisition (bathymetry, acoustic profiling). The application field is dedicated to shallow water inspection up to 150m. depth. The operation requires a reduced logistic, composed of 2 operators and a small ship (rubber boat type).

Figure 1 : Taipan 2
©LIRMM-HYTEC

Figure 2 : Taipan 2, inside view,
©LIRMM-HYTEC

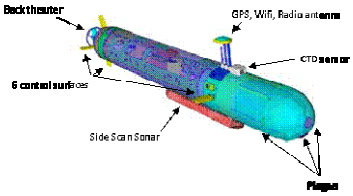

Figure 3 : Taipan 2 equipment
©LIRMM-HYTEC

According to the needs of the Meditate Project, the vehicle has been equipped with the devices, listed below:

General features

Weight	60 Kg
Length	2.1 m.
Diameter	20 cm.
Width with rudder	35 cm.
Height with antenna	35 cm.
Max Depth	160 m.
Max Speed	2 knots
Battery autonomy	2 hours
Materials	Aluminium, Delrin, Hostaform
Range	7.2 Km.

Batteries	48V
Propeller	Electric

Sensors

GPS	Trimble - Lassen SKII
Attitude Unit	Microstrain (3DM-G)
Loch Doppler	RDI, Workhorse 600
Pressure (2)	0 – 6 bars (0.1%), 0 – 16 (0.1%).
Side Scan Sonar	Tritech (325 – 675 KHz)
Digital Camera	Stortech (752(H) * 582 (V) pixels)
Echosounders (3)	Murata on NAVMAN 100
CTD Sensor	ADM

Communication devices

Radio UHF	Adcon (869.4 MHz)
Pinger (acoustic locator)	Benthos (25KHz)
Acoustic Modem	ORCA (33 KHz)
Wifi	DLink (2.4 GHz)

Electronic cards

Embedded PC Card	Advantech (1,26GHz P3, 512 Mo Ram)
Interface Card	LIRMM (8 RS232, 4 PWM, CAN/CNA)

Taipan 300

Taipan 300 is 1.8 m long and has a 15 cm diameter, for a total dry weight of about 30 kg. Its hull is completely watertight and trimmed at about 0.3 kg positive buoyancy (fig.4). The aluminum interface between the nose (made of hostaform) and the main carbon fiber body holds the bow diving plane (actuated by a servo-motor), the pressure sensor, the UHF and GPS antennas and the 10-pin underwater connector used to connect the onboard electronics with the outside The head (nose, interface) and all the electronic boards can be detached from the main body and all pop out as one. Watertightness is ensured by an O-ring and 6 screwnuts. A DC motor rotates the propeller via a gear wheel located outside the hull. The power electronics is located above the motor, next to the servo-motors used to actuate the rudder and the stern plane. The servo-motors command the rotation angles of axes through the hull. These angles are transmitted to the control surface axes via wire ropes. A fairing with fixed surfaces is located in front of the rudder and the stern plane. Behind the three-bladed propeller is a set of 4 fixed surfaces slightly twisted to stabilize the vehicle.

Figure 4 : Taipan 300


Figure 5 : Taipan 300, with Captain Jamal

The equipment onboard the Taipan 300 AUV is listed below:

General features

Weight	30 Kg
Length	1.7 m.
Diameter	15 cm.
Width with rudder	27 cm.
Height with antenna	30 cm.
Max Depth	100 m.
Max Speed	4 knots
Battery autonomy	1 hours
Materials	Aluminium, Carbon, Inox
Range	4.8 Km.
Batteries	24V
Propeller	Electric

Sensors

GPS	Trimble - Lassen SKII
Attitude Unit	XSens MTi
Pressure (2)	0 – 1 bars (0.5%), 0 – 10 (0.5%).
Echosounders (3)	Murata on NAVMAN 100D
CTD Sensor	ADM

Communication devices

Radio UHF	Satel Satelline 2ASxE (433 MHz)
Pinger (acoustic locator)	Benthos (25KHz)
Acoustic Modem	ORCA (33 KHz)
Wifi	DLink (2.4 GHz)

Electronic cards

Embedded PC Card	PC 104+ (400 MHz Celeron, 512Mo Ram)

Validation tests

Compass calibration

Two devices are able to estimate the system yaw angle, the RDI Loch Doppler and the Microstrain 3DM-G attitude sensor. We have proceeded to some tests far from electromagnetic sources in order to calibrate the yaw measurements (cf figure 6.a,b,c). These tests revealed the problematic internal location of the 3DM-G, which is interfering with other acoustic devices, and disqualified this sensor in the yaw measurement (fig 6.b). The RDI loch Doppler has been successfully calibrated, yielding the deviation table of the figure 6.c.

a. Test site

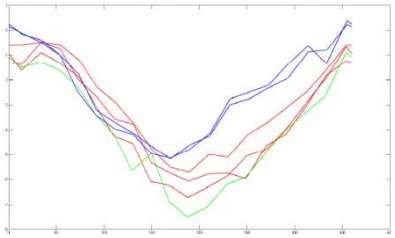

b. Measures in different conditions

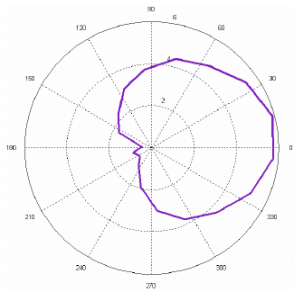

c. Compass Deviation

Figure 6 : compass calibration

Navigation Sensors suite validation

The first test campaign has been dedicated to the validation of the navigation sensors suite, in order to demonstrate and quantify the ability of the selected sensors to estimate the position of the vehicle along a pre defined path. In this scope, we have used a catamaran structure (figure 7) as a carrier to validate our sensor suite. This structure was linked on the LIRMM's boat (Bounty 2), and travelled along open loop trajectories. The onboard sensors are: a waterproof box containing the odometric sensor suite (attitude unit), the Side scan sonar and the Loch Doppler, and GPS receiver on the boat. The recorded GPS trajectory appears in light grey, and the estimated odometric trajectory appears in dark, on figure 8.

Figure 7: The catamaran structure for validation of the sensor suite. ©LIRMM-HYTEC

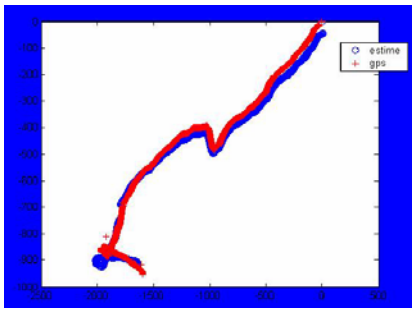

Figure 8: followed traj., GPS traj (grey), odometric traj. (dark)

CTD validation

In the scope of his master thesis, O. Laarman worked on the qualification of the CTD sensor. The conclusions are the following:

The measure of temperature with the CTD sensor has been compared with high precision thermometer measurements. These experiments allowed qualifying the validity of the CTD temperature measurements. Same method has been used to validate the conductivity measurements. Due to technical problems, the pressure sensor has not been qualified during these tests. The main results are displayed in Table 1.

Conductivity 25° (mS/cm)			Temperature
CTD	Conductimeter 1	Conductimeter 2	
0.745	0.744	0.739	20.7
	0.745	0.742	22.5
	0.746	0.741	26.4
22.46	22.6	22.5	21.7
	22.4	22.3	26.3
50.24	50.6	50.2	22.2
	50.1	50	29

Table 1: comparison of CT measurements

Side Scan Sonar image acquisition

The Side Scan Sonar is a powerful instrument designed to survey large sea-bottom areas. This system is very sensitive and its tuning is a difficult process. We proceeded to different missions with the goal of tuning the SSS parameters. We end up with images as displayed in figure 9, acquired among the Vise water spring in the Thau lagoon, and along the trajectory displayed in figure 5.a.

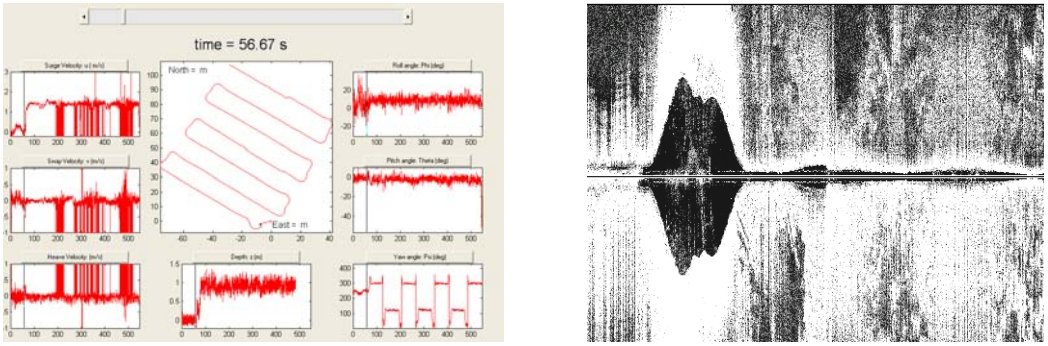

a. Mission analysis interface b. Acquired Side Scan Sonar image

Figure 9 : Side Scan Sonar Acquisition

Vehicle preliminary test

The sensors suite has been mounted on the Taipan 2 vehicle, with a Sliding Mode controller, in order to follow a pre defined horizontal trajectory with a constant desired depth.

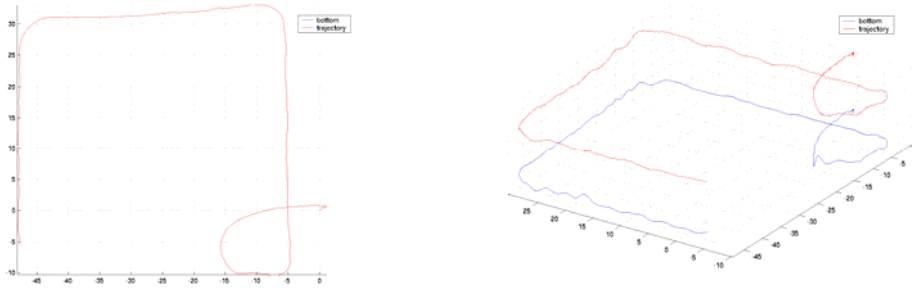

a. horizontal trajectory b. 3D trajectory

Figure 10: Taipan 2 following a square trajectory

They were conducted in the Thau Lagoon (Balaruc les Bains, France). Two examples of trajectories are given in the following figures (6 and 7).

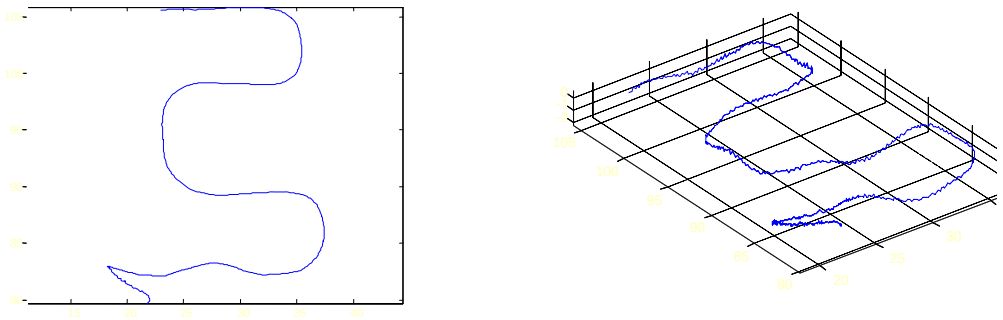

a. horizontal trajectory b. 3D trajectory

Figure 11: Taipan 2 following a regular survey trajectory, with CTD acquisition.

The CTD sensor has been recruited during the second test. We have obtained the measurements reported at figure 8, along the trajectory reported at figure 12.

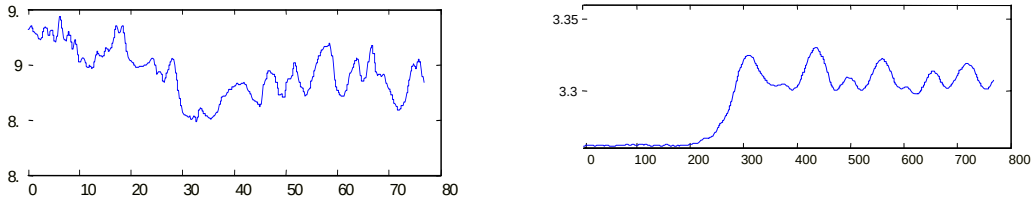

a. Measured temperature along the traj. (°) b. Measured salinity along the traj. (mg/l)

Figure 12: CTD measurements along the trajectory of figure 7.

Vehicle navigation validation

The navigation system validation requires comparing the results of the position estimation with some external positioning system, in order to consider the whole chain of data treatment and evaluate its performance. Tests were carried out in the Thau Lagoon and the Gulf of Hyères, in collaboration with the French company ACSA, specialised in GPS underwater systems. ACSA is developing the GibLite System that is able to real-time locate on a geo-referenced map an acoustic emitter mounted on a moving object. The GibLite system is composed with 4 floating devices (figure 13.a)

equipped with GPS receivers, able to triangulate the 3D position of the pinger, mounted on the vehicle, (figure 13.b).

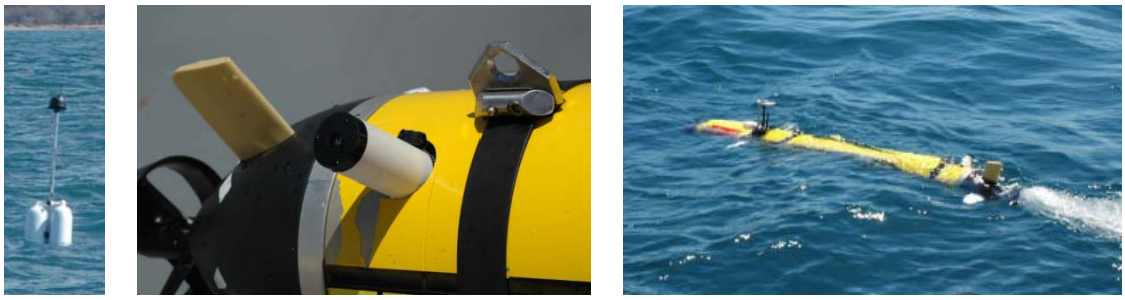

a. b. c.

Figure 13: Taipan 2 and the GibLite system ©LIRMM-HYTEC

At the end of each run, the GibLite system provided a geo-referenced estimation of the system trajectory (Figure 14). We used these data, to qualify or correct the navigation system estimation.

a. b. c.

Figure 14: Taipan 2 and the GibLite system ©LIRMM-ACSA

These tests revealed a remaining compass calibration error, but confirmed the accurate estimation of the linear velocity thanks to the RDI Loch Doppler.

Complete mission validation

Since the previous qualification tests have been successfully done, Taipan 2 has been used to complete different type of missions in various environments.

The Morgat Bay, France

The vehicle was deployed in the scope of the Explora exhibition, and made some demonstration about the efficiency and the feasibility of using a small AUV in the scope of mine detection or rapid environmental assessment. In this occasion, we showed that Taipan 2 is able to follow a long desired geometrical pattern during a 30 minutes mission. The horizontal trajectory (figure 15) clearly indicates the presence of the sea current, pointing south

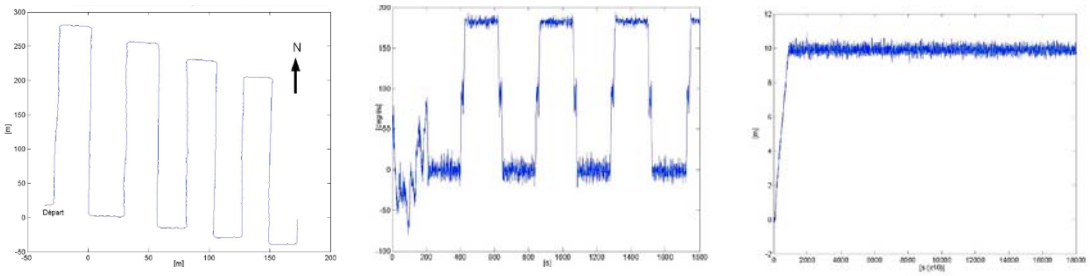

a. horizontal trajectory b. heading evolution c. depth control

Figure 15: the Morgat tests

La Spezia, Italy

Recently, Taipan 2 has been called to be involved in a demonstration for NATO in order to prove the efficiency of a small AUV equipped with Side Scan Sonar in the scope of anti-mine warfare. Taipan 2 was planned to reproduce the previous pattern (demonstrated in Morgat) acquiring Side Scan Sonar images along the trajectory. Unfortunately, a technical problem cancelled the mission and only the first pattern element was achieved. The figures 16.a,b,c. show the bathymetry, conductivity and temperature profile along the trajectory

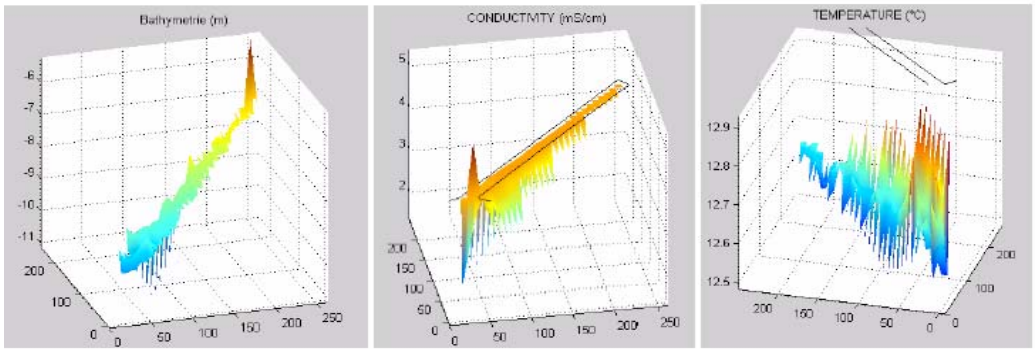

a. Bathymetry b. Conductivity profile c. Temperature profile

Figure 16: the La Spezia tests, CTD acquisition

The figures 17.b displays the SSS image acquired along the trajectory, clearly indicating a suspicious immerged object, that could be an underwater mine. The location of the detection is:

Echo detected at 31753.74s (mission time): 8h49.13 UTC

- 10°04’69.74” East
- 44°00’76.51” North

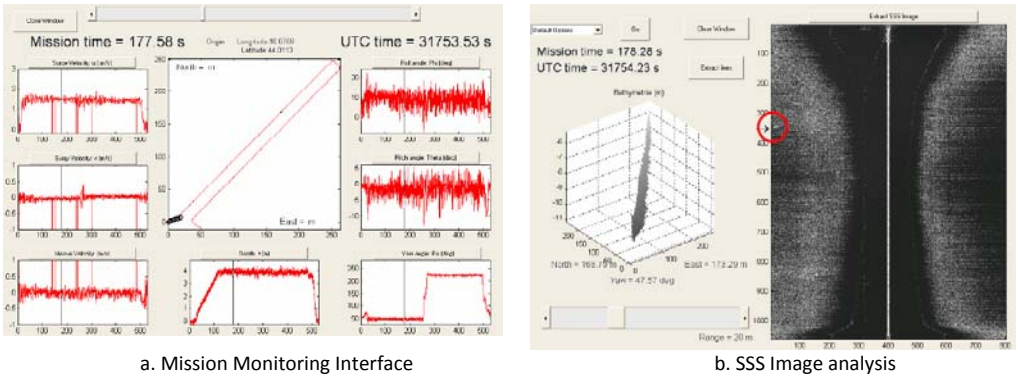

a. Mission Monitoring Interface b. SSS Image analysis

Figure 17: the SSS image acquired along the trajectory

This mission allowed for demonstrating the detection of such suspicious objects, and its location them on a geo-referenced map.

Man Machine interface specifications

As reported in the Deliverable 3, titled "Man-Machine Interface Specification", the MMI development is a whole discipline in itself, concerning the study of communication between machines and humans. The communication needs cover different aspects, according to the user objectives:

- The system designer has to access to low level information in order to test and validate the material and software architectures.
- The control developer has to integrate and tune its solutions, in terms of navigation, guidance, control, path planning… that requires an access to the installed module parameters.
- The low level mission controller designer is proposing some modules combinations in order for the vehicle to perform low level sub-objectives, i.e. dive, surface, join points A to B, recruit scientific sensor, travel at a desired depth….
- The end-user has to program the mission in understandable terms according to its scientific speciality. The mission aggregates the defined sub-objectives.
- And at last, the MMI has to include the on line system supervision module according to the permanent communication capabilities.

The system designer point of view

The system architectures (material and software) describe the organisation of the system organs (sensors and actuators), the electronic components (computers, Input-Output interface cards, communication medium) and the software architecture projected on the technological target. The qualities of these architectures are their modularity, determinism, and the ability to perform low level self diagnostic. Figure 18.a displays a synoptic view of the onboard architecture of Taipan 2.

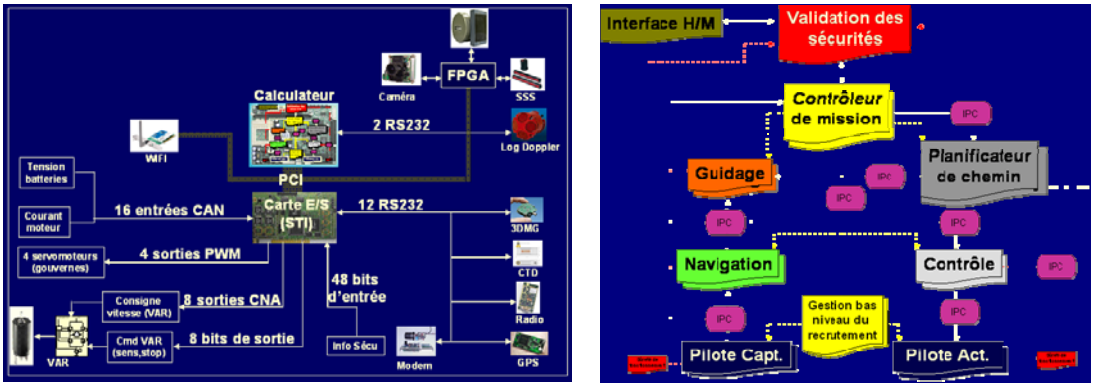

a. Hardware Architecture of Taipan 2 b. Software Architecture of Taipan 2

Figure 18: the Hardware and Software architecture of Taipan 2

During the conception, the designer has to validate and test all the system components. From its point of view, the MMI displays the component and the overall system states. During the mission, the required information to display is the result of the overall system diagnostic, that validates (or not) the ability of the system to perform the

mission in a safe manner. The software architecture is projected onto the system hardware architecture. In an optimal way, these both architectures should be totally independent. Nevertheless, the system reality and the lack of a generic architectures description impose to specialise the software architecture according to the system specifications. Figure 18.b shows a schematic view of the software architecture onboard Taipan 2.

The software modules need to be tested, in terms of time response and determinism. From the designer point of view, the MMI displays the test results of the software modules and a validation of the IPC components.

The control designer point of view

The control developer proposes solutions that have to be integrated in the modules Navigation, Guidance, Control and Path planner. Generally these solutions require gains tuning that have to be available for the developer. Each module needs a parameter board included in the MMI. Figure 19 displays the parameter tuning board for the Sliding Mode Control used for Taipan 2.

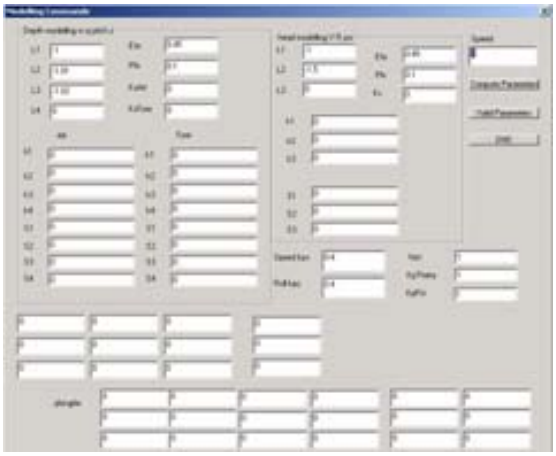

Figure 19 : the control parameters tuning board of Taipan 2

The low level mission controller point of view

The mission is composed of sub-objectives that have to be executed in a sequential or event based way. The sub-objectives description belongs to the low level mission scheme. A generic sub-objective requires the creation of a set of primitives, aggregated to compose the whole mission description. These primitives concern the organs recruitment, elementary actions like ‘dive’, ‘surface’, ’desired yaw control’, ‘follow the defined path’ (this needs a path definition by the user), ‘desired region joining’ (this requires a region definition by the user), ‘acquire specific sensor information’,… The goal of this part of the MMI, is the primitives definition.

The low level mission controller designer needs to test, validate all the defined primitives and create new ones. Each of the primitive requires a parameter board. Figure 20 shows the primitive interface testing for Taipan 2 (20.a) and Taipan 300 (20.b)

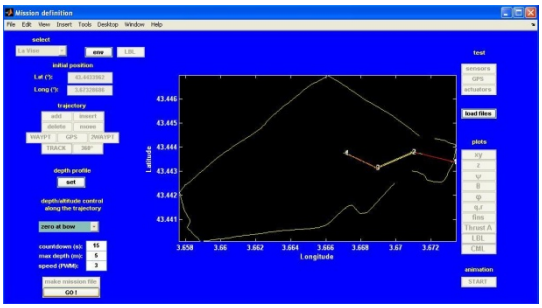

a. The Taipan 2 mission interface

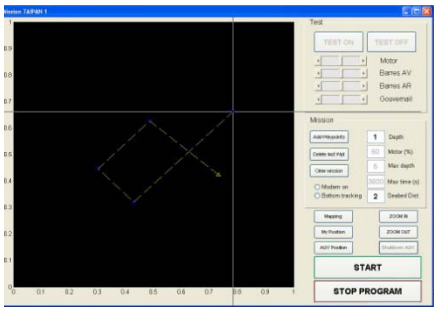

b. The Taipan 300 mission interface

Figure 20 : mission interfaces developed at LIRMM.

The supervision module

During the system deployment, basic system information could be on line displayed, in function of the permanent system communication devices, as acoustic modem, or radio link for a sporadic contact (requires being at surface). These informations include the system state, the security layer state… Figure 21 displays example of supervision modules for the vehicles AUV-Infante (IST) and ASC-Delfim (IST).

a. The Delfin (IST) supervision module

a. The Infante (IST) supervision module

Figure 21 : examples of supervision modules

The end-user point of view

The end user has to define the mission. The previous considerations are transparent for him. The MMI provides a set of primitives, defined in function of the end-user speciality. In our case, the end-user has a hydro geologist background and is using the vehicle to acquire physico-chemical samples of the water along the trajectory. The figure 6 displays an example of a user path definition. With another aggregation level, the MMI provides a geo-referenced map of the area where the vehicle has to operate. This allows the end-user to define a region of interest where the vehicle has to acquire the desired scientific information. Then the vehicle has to reach the desired region from its current location, acquire the data, and return back to a predefined meeting point. Figure 22 displays an example of the end-user mission programming module, developed at IST.

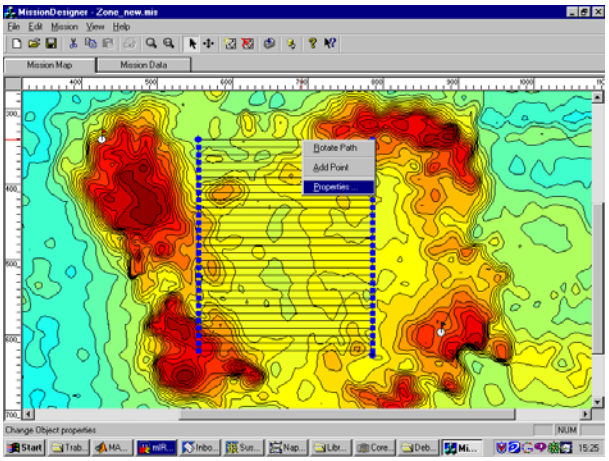

Figure 22 : Example of End-user mission programming module (IST)

Specification of an end-user mission programming interface for hydrogeologists

The end-user interface proposes elements to define the mission, in understandable terms for hydrogeologist, hiding all the lower levels of the vehicle control. The interface is displaying a map of the working area. The map scale should include both coordinates systems:

- Metric, Lambert 2 or 3 (France)
- Latitude, Longitude GPS classic geo-reference

This map could be enriched with all the available *a-priori* terrain knowledge

- Previously acquired bathymetric map
- IGN map
- Possible bridge with the software MapInfo and ArcView

The user is invited to select on the map a region of interest where the sample will be carried out. This implies choices selected by the user:

- Propose a path to join the region, confirmed or redrawn by the user
- Propose a path to sample the region
    - Regular grid
    - Cycloids
    - User defined, with waypoints
- Define an end of mission meeting point
    - Propose a path to join the meeting point
    - User defined
- Select a desired depth for the path
    - Constant depth
    - Bottom following with a desired altitude
    - User defined, with waypoints
- Select a sampling precision, that has an incidence on the vehicle forward velocity, in function of the sensor sampling rate
- GPS calibration points for dead reckoning navigation.
    - Automatic
    - User defined

The user could also be invited to select points of interest in the working region:

- Proposition of a compatible path, confirmed or redrawn by the user.

- Define an end of mission meeting point
    - Propose a path to join the meeting point
    - User defined
- Select a desired depth for the path
    - Constant depth
    - Bottom following with a desired altitude
    - User defined, with waypoints
- Select a sampling precision.
- GPS calibration points for dead reckoning navigation.
    - Automatic
    - User defined

Another interesting possibility of the vehicle is to perform a sensor based control to navigate in order to minimize a define criterion, in a defined region of interest.

- Propose a path to join the region, confirmed or redrawn by the user
- Selection of the criterion
    - Isothermal navigation,
    - Temperature gradient minimization / maximization
    - Salinity isocline navigation
    - Salinity gradient minimization / maximization
- Select a sampling precision, that have an incidence on the vehicle forward velocity, in function of the sensor sampling rate
- Safe depth/altitude definition
- Select a reaction in case of
    - Surfacing
    - Exceeding the safe depth
    - Exceeding the safe altitude
    - Leaving the defined region of interest
- Define an end of mission meeting point
    - Propose a path to join the meeting point
    - User defined
- Define the stopping criterion
    - Temporal
    - Spatial
    - User-defined
- GPS calibration points for dead reckoning navigation.
    - Automatic
    - User defined

The previous mission primitives include hidden subroutines that have to be sequentially performed by the system.

Mission analysis module

Once the mission is done, one could be able to easily proceed to a clear results interpretation. In this scope, we have developed an interface allowing for 2D and 3D plotting the acquired samples during the mission. These samples have to be geo referenced in order to precisely locate the acquisition region. Figure 17 displays the modules allowing for replaying the mission and analysing the Side Scan Image, with the classic waterfall view. Figure 23 displays the mission analysis module we have developed for the mission done in Gökova Bay (Turkey)

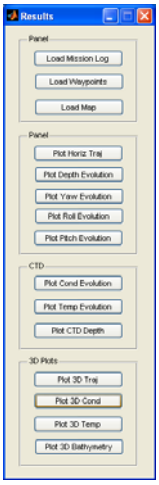

a. Analysis module, main frame

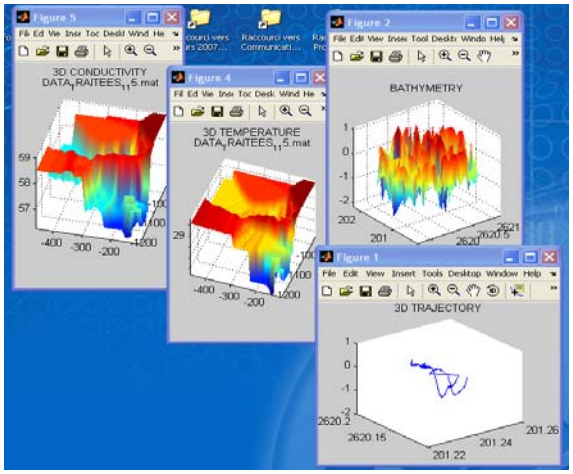

b. different view of the 2D and 3D plotting of the acquired data

Figure 23 : the Analysis module developed for Meditate.

Data Fusion

The data fusion process should allow for exploiting the acquired samples in a rigorous and easy-to-use way. We have designed the fusion module using the software Matlab. After running a mission , the vehicle records are the following :

- The estimated system 3D trajectory.
- The GPS fixes done when the vehicle is at surface.
- The conductivity and temperature samples acquired along the trajectory.
- The vertical distance to the sea-bottom.

These data needs to be post-treated in order to obtain an accurate geo-reference of the acquired samples, in order to locate them in an absolute frame.

Computing the system trajectory

The online estimation of the system trajectory is made according to the starting point of the mission. The use if the navigation sensors (attitude unit and DVL Log Doppler) allows for computing an estimation of the system current position, given the system velocities, the current depth and yaw angle. Indeed this type of estimation presents a drifting error that is increasing with time. This implies for the system to regularly reach the surface in order to acquire a GPS fix, and calibrate the position, resetting the drifting error to 0. This treatment is made on line, onboard the system. Nevertheless, an off-line smoothing process is necessary in order to reduce the drifting error to the minimum.

Data association

Once the trajectory computation is done, the data association allows for attributing to the conductivity and temperature samples an estimation of the geo-referenced location. This association is made according to a common temporal reference that is indexing all the measurements, including the navigation information.

Plotting the results

The final results require to be displayed on a georefenced map with different type of views. Indeed, the temperature and conductivity are displayed on different depth, using a 3D view (figure 24.a) or a colored 2D view showing the geographical region of the samples (figure 24.b).

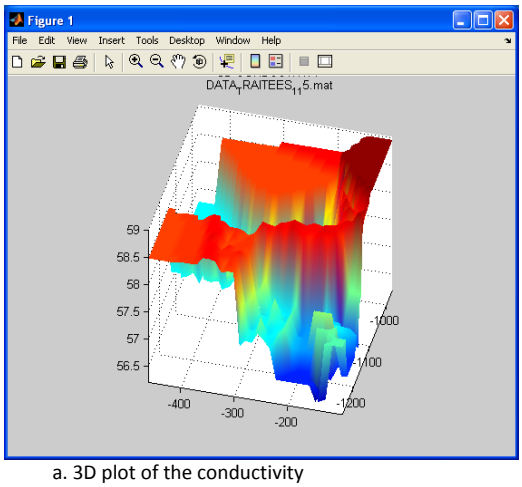

a. 3D plot of the conductivity

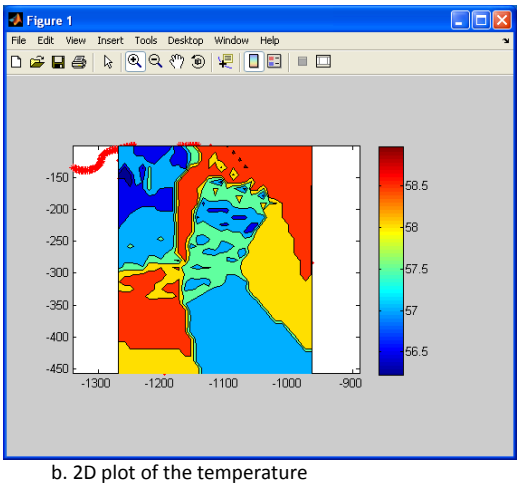

b. 2D plot of the temperature

Figure 24 : different views of the geo-referenced conductivity measurements at a given depth

We display in the following section the results we have obtained during our missions in La Vise (Balaruc les Bains, France), and Gökova Bay (Gökova, Turkey).

AUV missions

In the scope of the Meditate Project, we are done several missions on two different sites: La Vise (Montpellier, France) and Gökova Bay (Gökova, Turkey). The geo-political situation of the Lebanese and Syrian regions did not allowed us to perform the desired runs on these promising sites. Nevertheless, the great interest of these sites pushes to consider and program future missions in order to push further the fundamental subject of the Meditate Project. The location of the envisaged study areas are displayed in Figure 25.

Figure 25 : The Study areas

La Vise (Montpellier, France)

The fresh underwater spring La Vise is located in the Thau Lagoon, nearby the city of Balaruc les Bains, south of France (Figure 25). As displayed on Figure 26.a the fresh water plume is visible from the shore, and the resurgence depth is about 36 meters, located at the bottom of a 80-meter diameter cone, and rising up to a depth of 2 meters (cf. Figure 2).

a. View of the plume reaching surface (M. Bakalowicz)

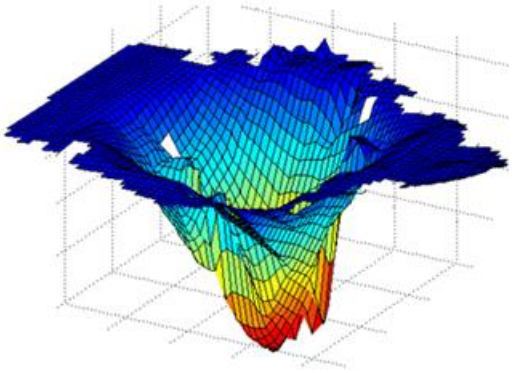

b. Bathymetry of the spring La Vise

Figure 26 : La Vise

In collaboration with the ACSA Company, we made a complete survey of the Vise water spring in the Thau lagoon, using the Taipan 2 vehicle. 4 different vehicle runs were conducted, with the GibLite system allowing for checking for appropriate geo-referencing. The 4 runs flew over the water spring (Figure 27), and allowed for significant CTD data acquisition.

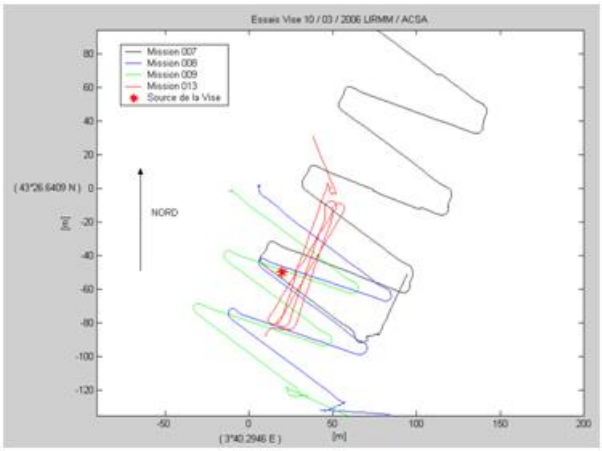

Figure 27: the 4 runs over the Vise water spring

The data fusion process, allowed for bathymetry, conductivity and temperature mapping, using the data acquired during the 4 runs (Figure 28.a,b,c).

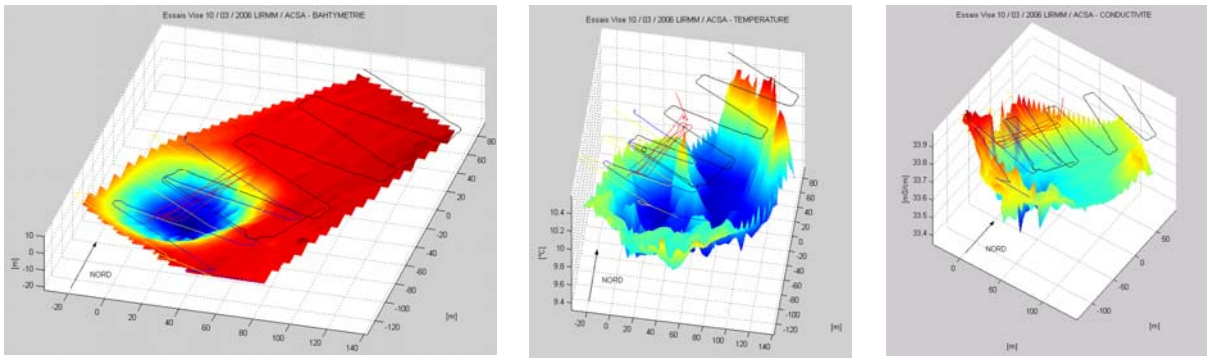

a. Bathymetry 3D mapping b. Temperature 3D mapping c. Conductivity 3D mapping

Figure 28: the 4 runs 3D data fused on a geo-referenced map

The superposition of these graphics along the horizontal plane clearly indicates the centre of the source as a minimum of depth, temperature and conductivity (Figure 29.a,b,c).

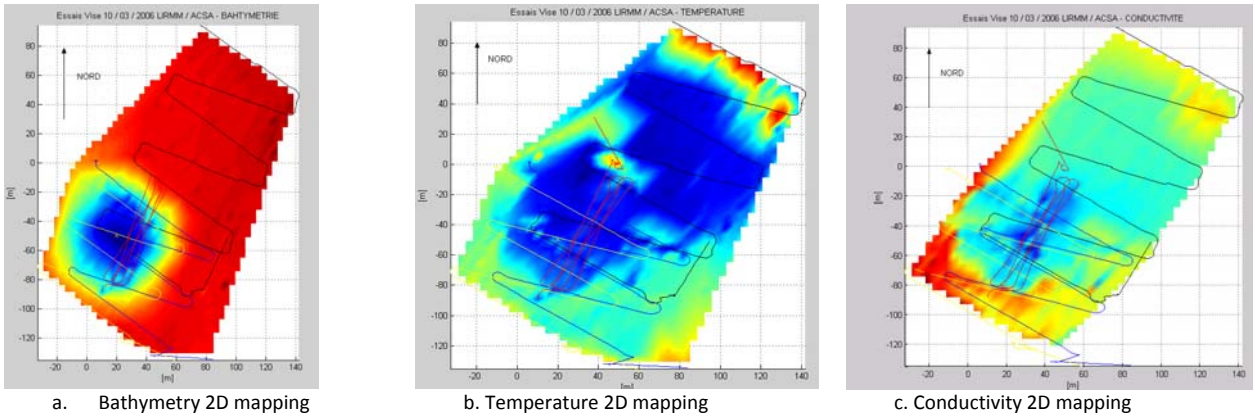

a. Bathymetry 2D mapping b. Temperature 2D mapping c. Conductivity 2D mapping

Figure 29: the 4 runs 2D data fused on a geo-referenced map

Gökova Bay (Gökova, Turkey)

The survey mission of the Gökova Bay took place between the 28/07/2007 and the 3/08/2007, using the Taipan 300 vehicle (Figure 30).

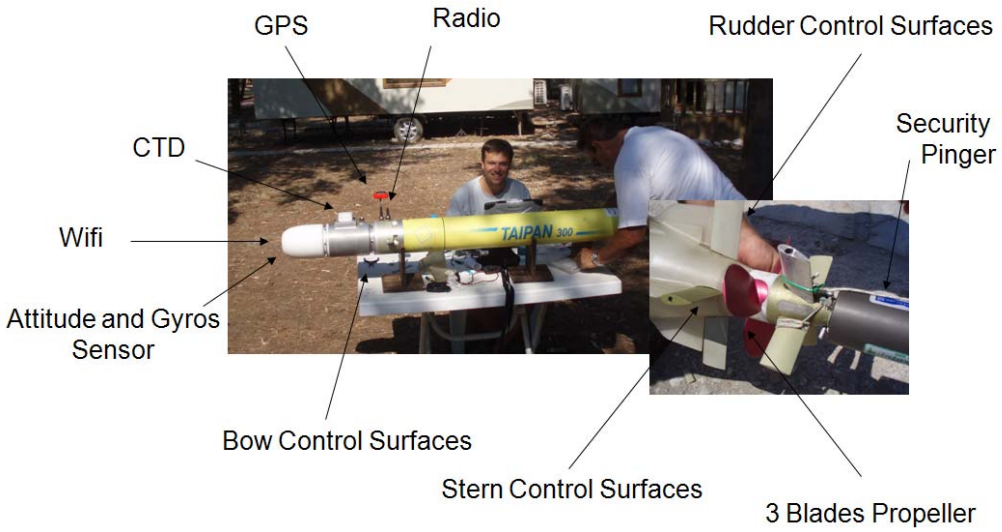

Figure 30 : The Taipan 300 AUV, reassembled in Gökova.

Unfortunately, the transportation made the AUV suffering, and the most part of the time during the mission was dedicated to the reparation of the successive breakdowns encountered during the missions (Figure 31).

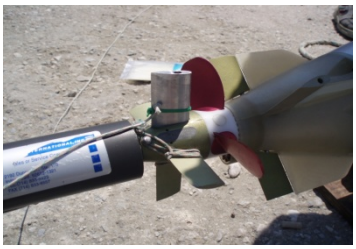

a. Emergency repair after the loss of a stabilizer.

b. Analysis of the internal heating problem.

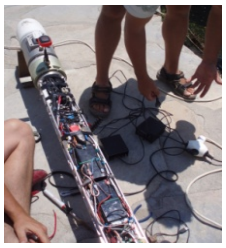

c. Replacing the defective wires

d. Replacement of the batteries

e. Finishing the reparation in the hotel room

f. Emergency calibration of the attitude unit

Figure 31: Emergency repairs of the AUV.

Regarding to the relative reliability of the machine, we decided to focuse the survey over a restricted zone, described in figure 31.a. The Figure 31.b displays a view of a fresh water plume reaching the surface. The Gökova Bay presents a large number of these

intrusions all along the shore. The location of these springs being very close to the shore, the runs were executed starting far from the shore, and getting closer.

a. Gökova Bay, geographical tests location

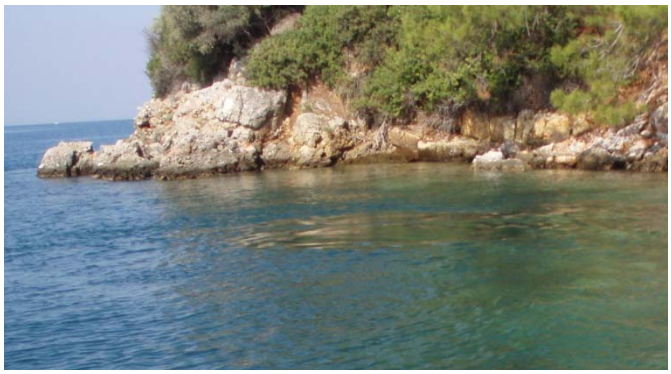

b. view of the plume reaching surface

Figure 31: the restricted test zone

Day 1

During the first day at sea, we first acquired a local geo referenced map, in order to locally program the desired runs. The acquired map is displayed on Figure 32.a. We launched the AUV for 9 runs; the significant trajectories are displayed on Figure 32.b.

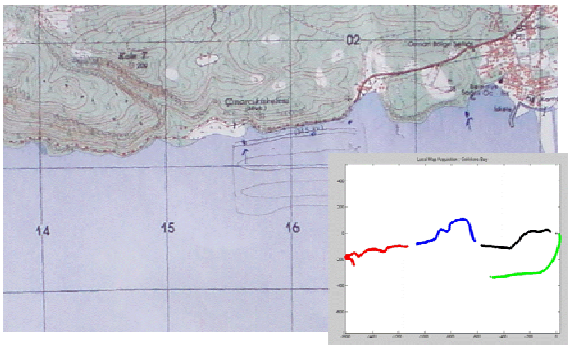

a. Local map acquisition

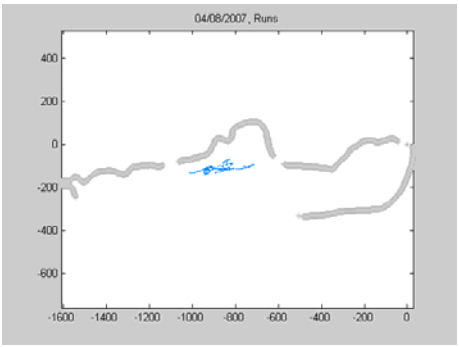

b. Significant trajectories of Day 1

Figure 32: the first day runs at sea.

The main results of these runs were to identify the electronical and mechanical problems of the machine.

Day 2

The second day was luckier, and we end up with 9 significant runs, displayed in Figure 33.

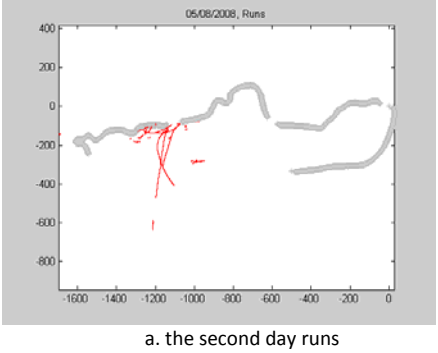

a. the second day runs

b. The onboard happy team

Figure 33: the second day at sea.

Data fusion

We finally fuse all the acquired data over the 9 significant runs. In order to cope with the desired analysis we sorted the data in function of the depth where the data have been acquired. The sorting was made for each 50 cm depth, and the results are presented below.

1. Samples acquired between 0 and 0.5m depth.

Results display : 0 – 0.5 m.
304 samples
30 measurements
Average temperature : 28.09°
Average Conductivity : 54.14 mS/cm

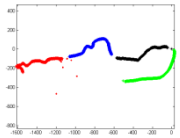

a. Geographical location of the samples

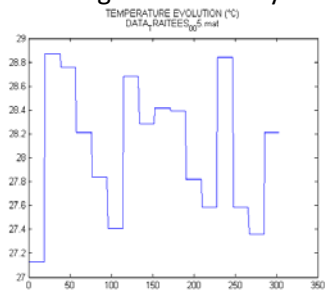

b. Temperature evolution

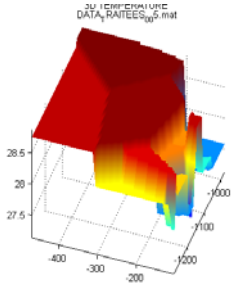

c. elevation map of the temperature

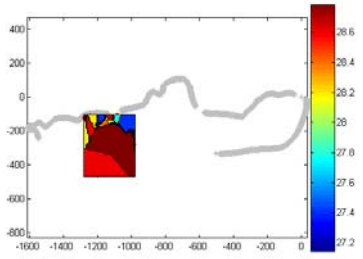

d. Geo referenced 2D map of the temperature

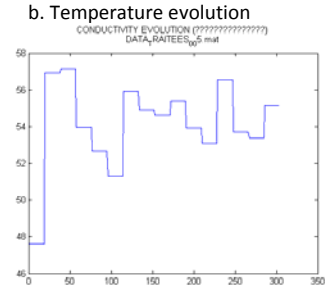

e. Conductivity evolution

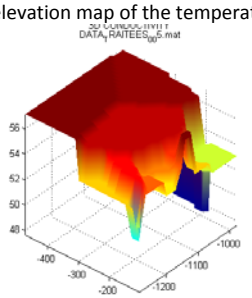

f. elevation map of the conductivity

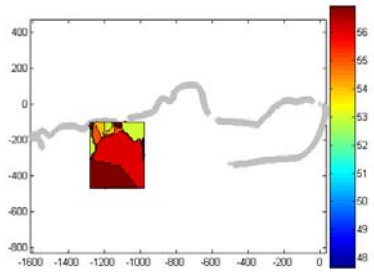

g. Geo referenced 2D map of the conductivity

Figure 33: Results of the samples acquired between 0 and 0.5m depth

2. Samples acquired between 0.5 and 1m depth.

Results display : 0.5 – 1 m.
931 samples (93 measurements)
Average temperature : 28.94°
Average Conductivity : 57.55 mS/cm

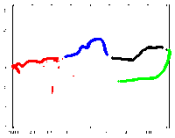

a. Geographical location of the samples

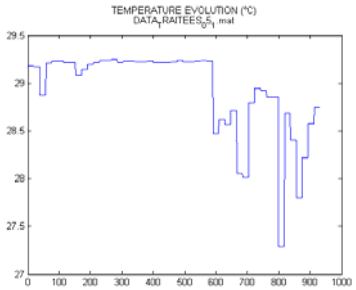

b. Temperature evolution

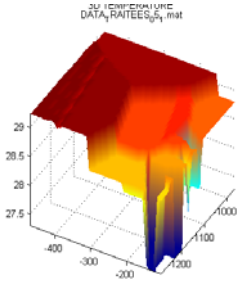

c. elevation map of the temperature

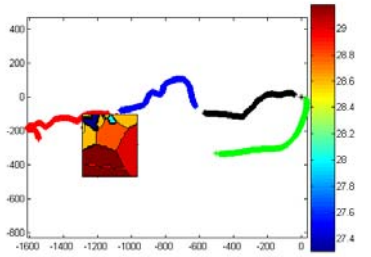

d.Geo referenced 2D map of the temperature

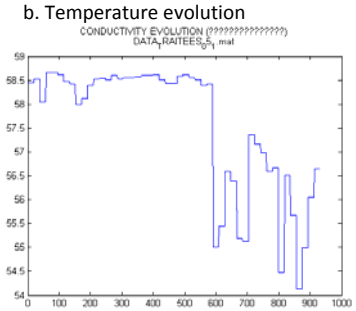

e. Conductivity evolution

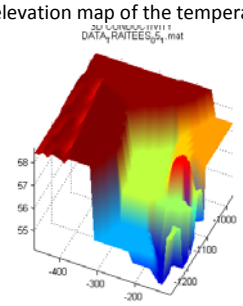

f. elevation map of the conductivity

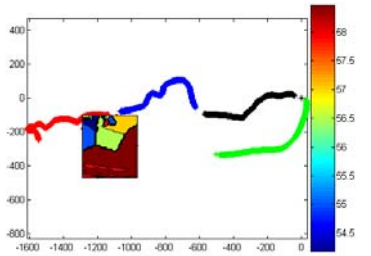

g. Geo referenced 2D map of the conductivity

Figure 34: Results of the samples acquired between 0.5 and 1m depth

3. Samples acquired between 1 and 1.5m depth.

Results display : 1 – 1.5 m.
5283 samples (528 measurements)
Average temperature : 29.06°
Average Conductivity : 57.93 mS/cm

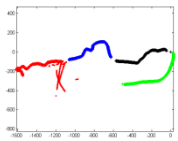

a. Geographical location of the samples

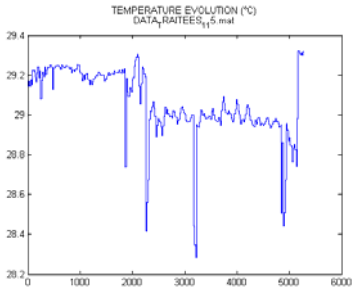

b. Temperature evolution

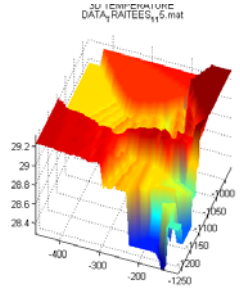

c. elevation map of the temperature

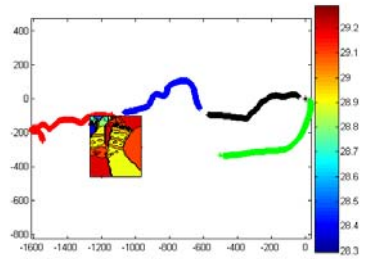

d. Geo referenced 2D map of the temperature

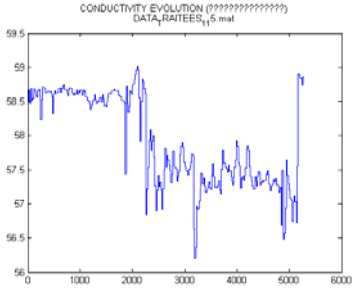

e. Conductivity evolution

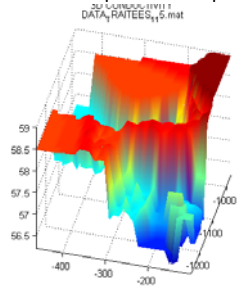

f. elevation map of the conductivity

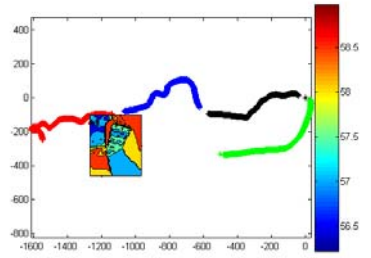

g. Geo referenced 2D map of the conductivity

Figure 35: Results of the samples acquired between 1 and 1.5m depth

4. Samples acquired between 1.5 and 2m depth.

Results display : 1.5 – 2 m.
729 samples (72 measurements)
Average temperature : 29.10°
Average Conductivity : 58.17 mS/cm

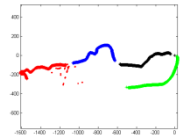

a. Geographical location of the samples

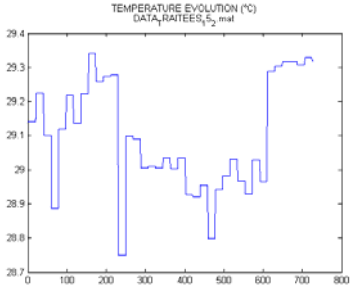

b. Temperature evolution

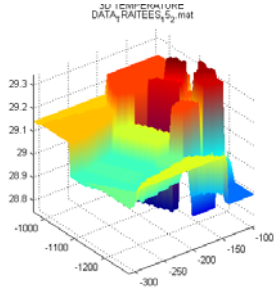

c. elevation map of the temperature

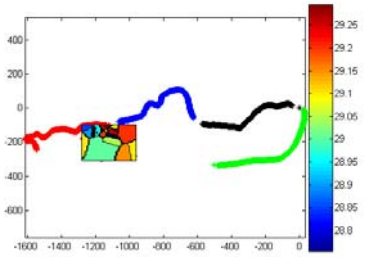

d. Geo referenced 2D map of the temperature

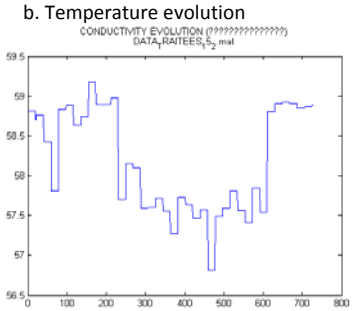

e. Conductivity evolution

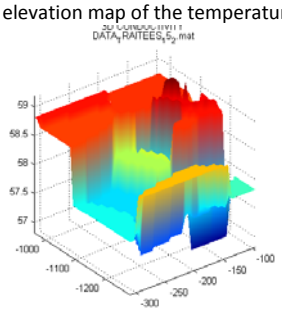

f. elevation map of the conductivity

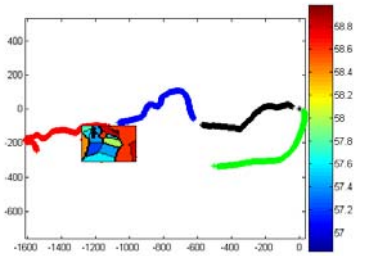

g. Geo referenced 2D map of the conductivity

Figure 36: Results of the samples acquired between 1.5 and 2m depth

5. Samples acquired between 2 and 2.5m depth.

Results display : 2 – 2.5 m.
394 samples (39 measurements)
Average temperature : 29.18°
Average Conductivity : 58.76 mS/cm

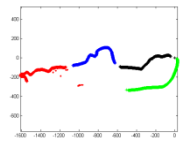

a. Geographical location of the samples

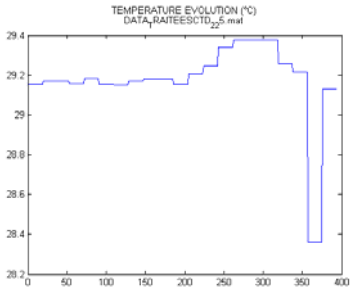

b. Temperature evolution

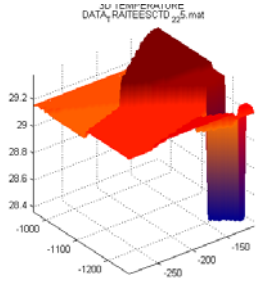

c. elevation map of the temperature

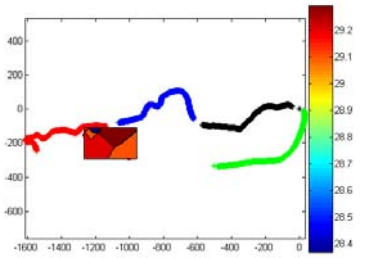

d. Geo referenced 2D map of the temperature

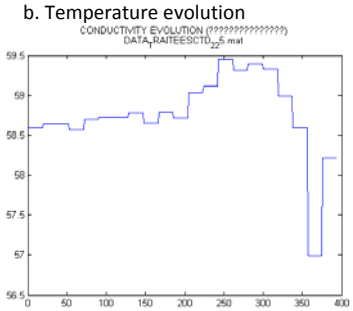

e. Conductivity evolution

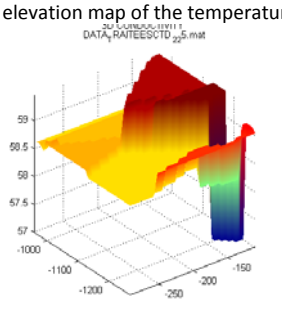

f. elevation map of the conductivity

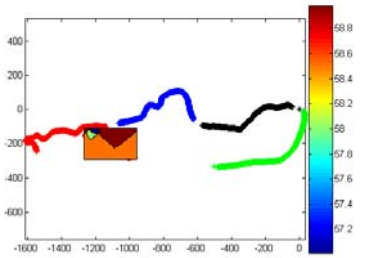

g. Geo referenced 2D map of the conductivity

Figure 37: Results of the samples acquired between 2 and 2.5m depth

6. Samples acquired between 2.5 and 3m depth.

Results display : 2.5 – 3 m.
190 samples (19 measurements)
Average temperature : 29.29°
Average Conductivity : 59.22 mS/cm

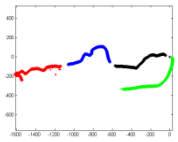

a. Geographical location of the samples

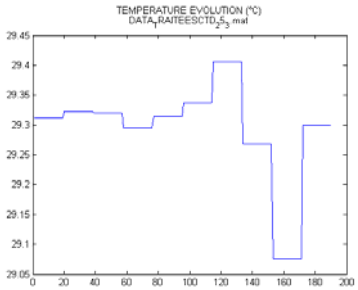

b. Temperature evolution

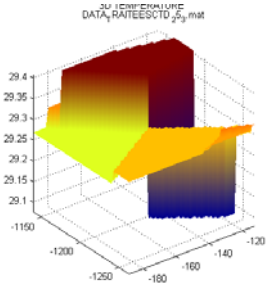

c. elevation map of the temperature

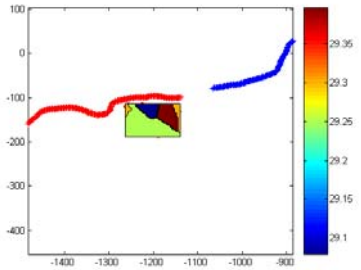

d. Geo referenced 2D map of the temperature

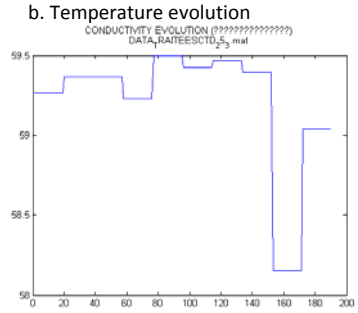

e. Conductivity evolution

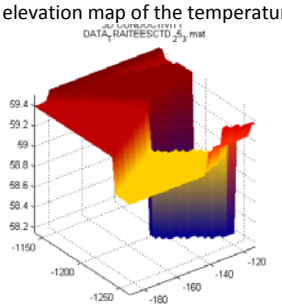

f. elevation map of the conductivity

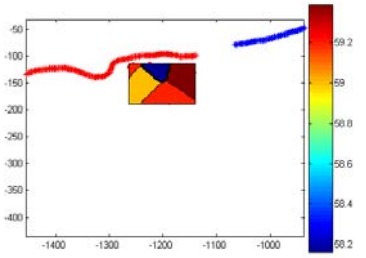

g. Geo referenced 2D map of the conductivity

Figure 38: Results of the samples acquired between 2.5 and 3m depth

7. Samples acquired between 3 and 3.5m depth.

Results display : 3 – 3.5 m.
131 samples (13 measurements)
Average temperature : 29.26°
Average Conductivity : 59.40 mS/cm

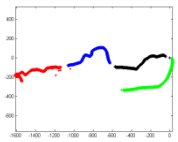

a. Geographical location of the samples

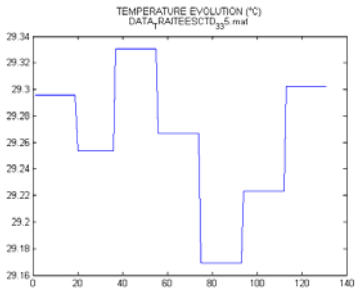

b. Temperature evolution

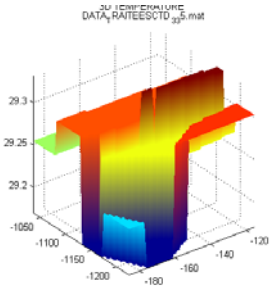

c. elevation map of the temperature

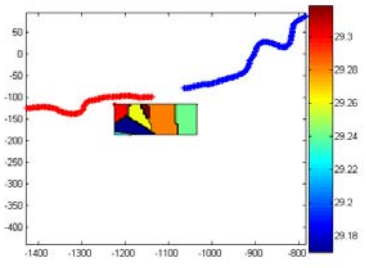

d. Geo referenced 2D map of the temperature

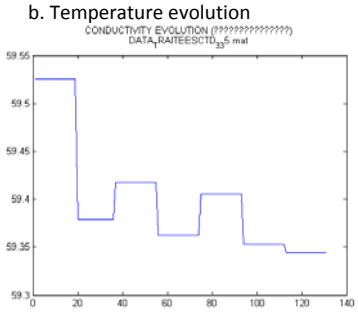

e. Conductivity evolution

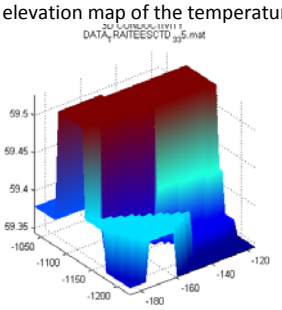

f. elevation map of the conductivity

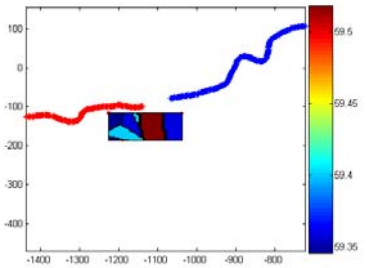

g. Geo referenced 2D map of the conductivity

Figure 39: Results of the samples acquired between 3 and 3.5m depth

8. Samples acquired between 3.5 and 4m depth.

Results display : 3 .5– 4 m.
85 samples (8 measurements)
Average temperature : 29.11°
Average Conductivity : 59.36 mS/cm

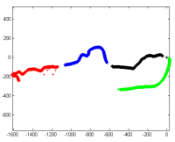

a. Geographical location of the samples

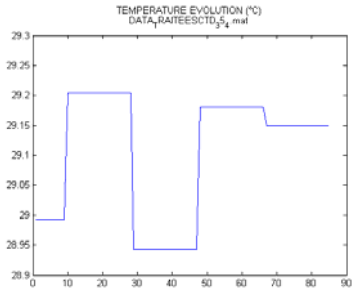

b. Temperature evolution

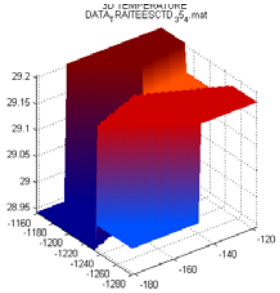

c. elevation map of the temperature

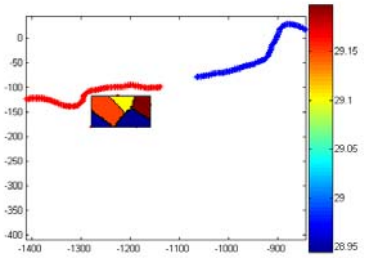

d. Geo referenced 2D map of the temperature

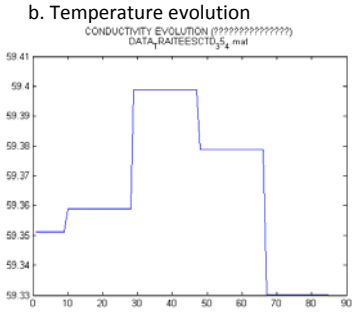

e. Conductivity evolution

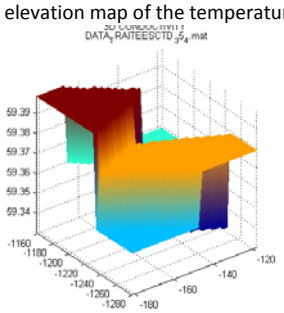

f. elevation map of the conductivity

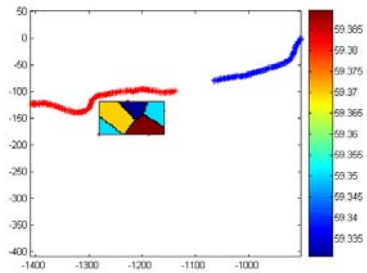

g. Geo referenced 2D map of the conductivity

Figure 40: Results of the samples acquired between 3.5 and 4m depth

9. Samples acquired between 4 and 4.5m depth.

Results display : 4– 4.5 m.
95 samples (9 measurements)
Average temperature : 28.05°
Average Conductivity : 58.49 mS/cm

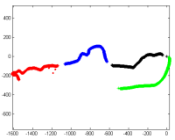

a. Geographical location of the samples

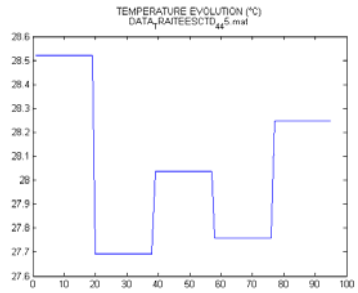

b. Temperature evolution

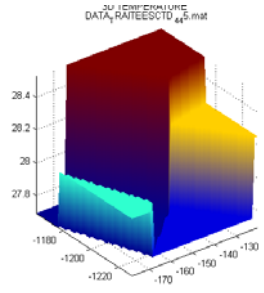

c. elevation map of the temperature

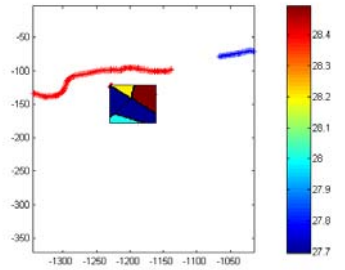

d. Geo referenced 2D map of the temperature

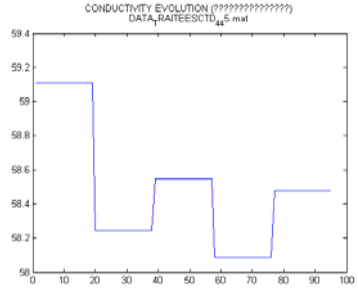

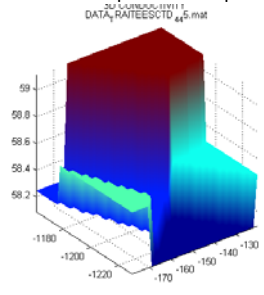

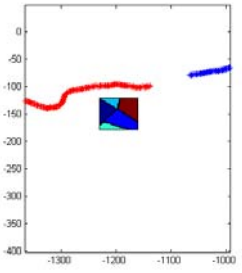

e. Conductivity evolution f. elevation map of the conductivity g. Geo referenced 2D map of the conductivity

Figure 41: Results of the samples acquired between 4 and 4.5m depth

10. Samples acquired between 4.5 and 5m depth.

Results display : 4.5– 5 m.

152 samples (15 measurements)

Average temperature : 27.62°

Average Conductivity : 58.07 mS/cm

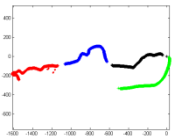

a. Geographical location of the samples

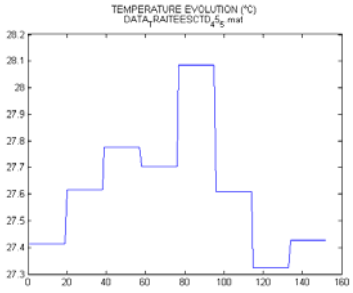

b. Temperature evolution

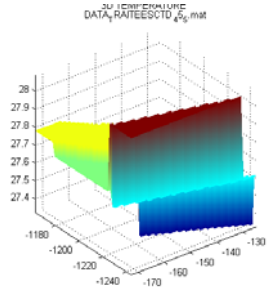

c. elevation map of the temperature

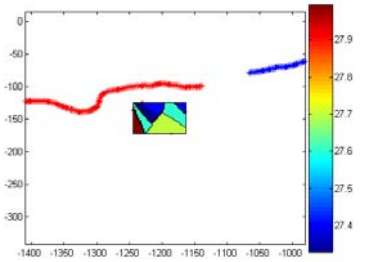

d. Geo referenced 2D map of the temperature

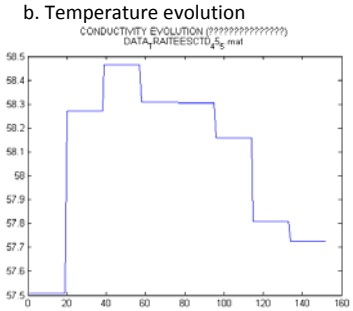

e. Conductivity evolution

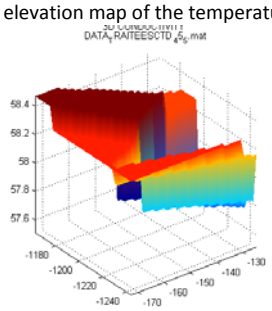

f. elevation map of the conductivity

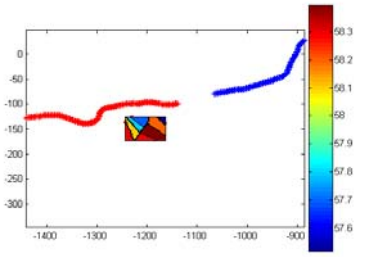

g. Geo referenced 2D map of the conductivity

Figure 42: Results of the samples acquired between 4.5 and.5m depth

11. Samples acquired between 5 and 5.5m depth.

Results display : 5– 5.5 m.

190 samples (19 measurements)

Average temperature : 27.74°

Average Conductivity : 58.57 mS/cm

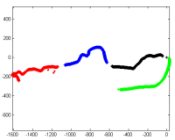

a. Geographical location of the samples

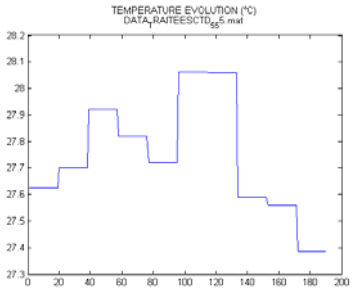

b. Temperature evolution

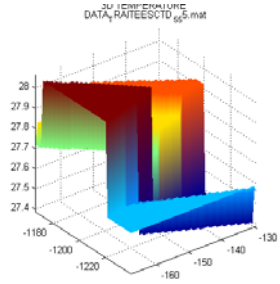

c. elevation map of the temperature

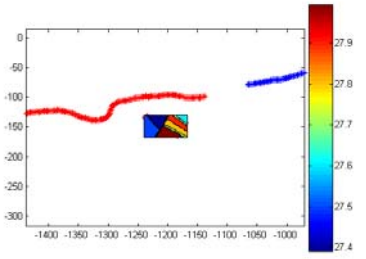

d. Geo referenced 2D map of the temperature

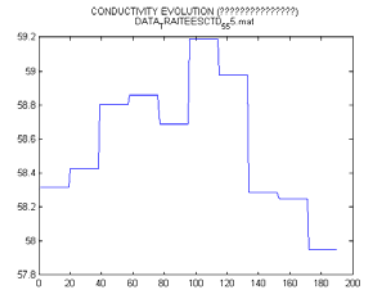

e. Conductivity evolution

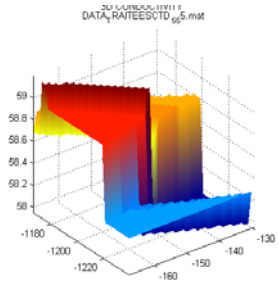

f. elevation map of the conductivity

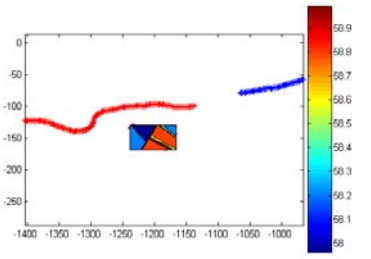

g. Geo referenced 2D map of the conductivity

Figure 43: Results of the samples acquired between 5 and.5.5m depth

12. Samples acquired between 5.5 and 6m depth.

Results display : 5.5– 6 m.
76 samples (7 measurements)
Average temperature : 27.77°
Average Conductivity : 58.75 mS/cm

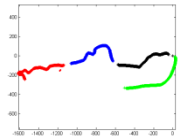

a. Geographical location of the samples

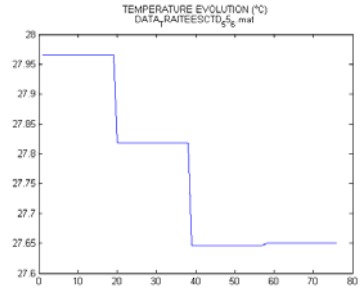

b. Temperature evolution

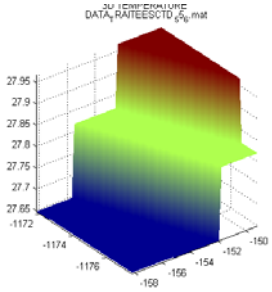

c. elevation map of the temperature

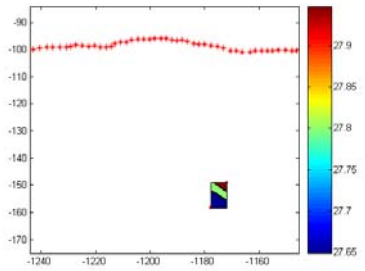

d. Geo referenced 2D map of the temperature

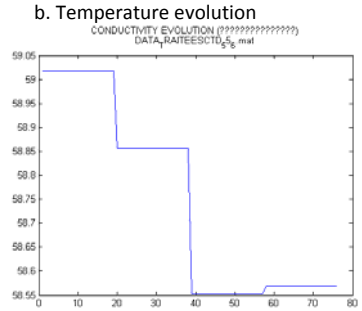

e. Conductivity evolution

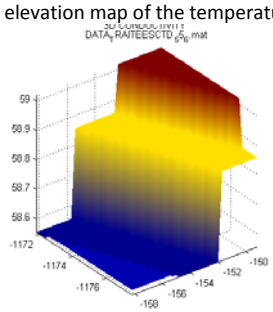

f. elevation map of the conductivity

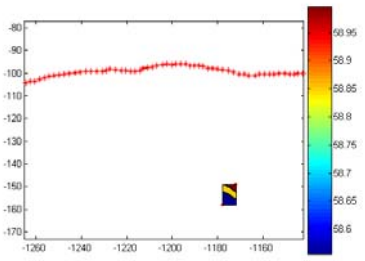

g. Geo referenced 2D map of the conductivity

Figure 44: Results of the samples acquired between 5.5 and.6m depth

Temperature gradient observation

In the following figure (Figure 45), we compare the observed gradient of the temperature (average temperature w.r.t. depth) with the classic expected gradient of the temperature at sea, without fresh water intrusion.

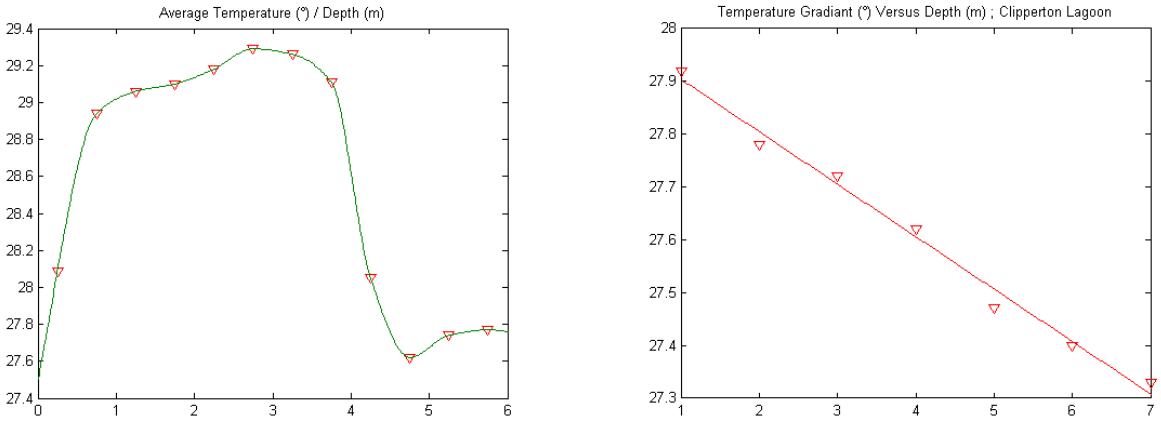

a. Observed temperature gradient in Gökova

b. Open sea measurements[1]

Figure 45: Comparison of the observed gradient with open sea measurements.

The comparison of the two curves of Figure 45 clearly indicates the intrusion of fresh water in the system. As observed *in situ*, the fresh water induces a decreased salinity and temperature at surface.

Detection of spring location

The next result (Figure 46) has been obtained in averaging the measurements along depth. This illustrate clearly the fresh water spring location

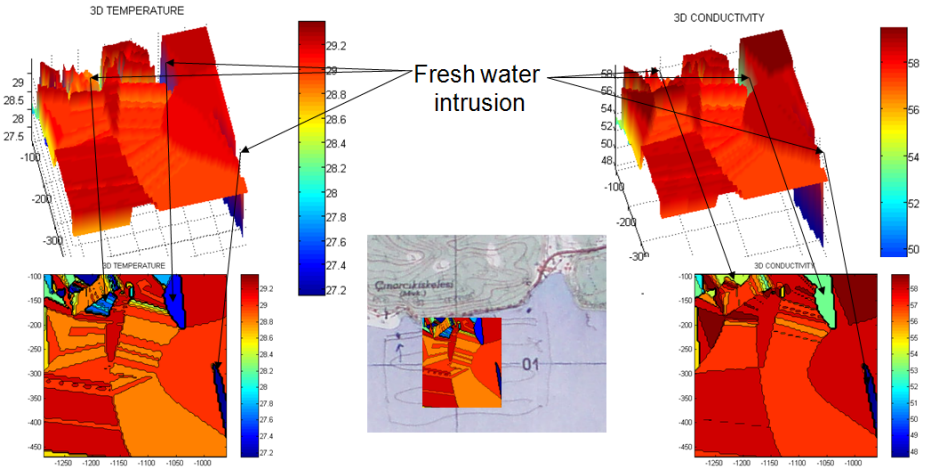

Figure 46: Fresh water spring detection

The fusion process allows for geo referencing this estimated location on the global map of the site, as illustrated in Figure 47.

[1] http://www.educnet.education.fr/clipperton),

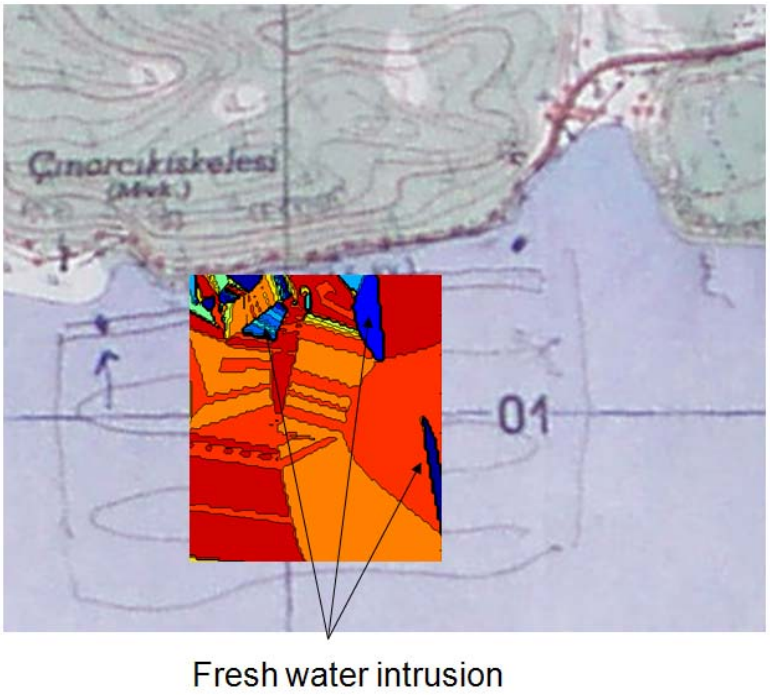

Figure 47: Fresh water spring location

Results on AUV control

Performing survey operation of an underwater spring using an autonomous vehicle might be a difficult task, in function of the local constraints. Indeed, the survey has to be done at different depth, in order to acquire a complete 3D sampling of the plume. This imply, in the context of the Vise spring to be able to dive in the cone (Figure 26.b) at different depths. Figure 48 displays an example of such desired trajectories.

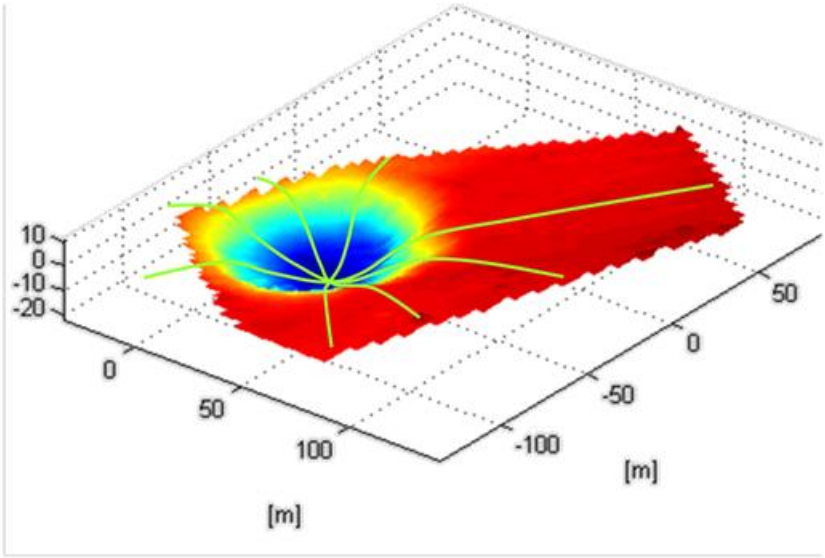

Figure 48: example of desired trajectories in order to dive in the cone of La Vise spring.

The control of the AUV during this type of mission, consisting in following the desired trajectories displayed in Figure 48, implies to be able to simultaneously control the horizontal plane (the yaw angle and the propulsion) and the diving plane (heave and pitch evolution). The concurrent control of the heave and pitch evolution induces some constraints on the AUV actuation. Indeed, only vehicle carrying bow and stern control surfaces will be able to achieve such a goal (Figure 49).

Figure 49: the full diving actuation of the AUV Taipan 2.

This actuation capacity induces a redundancy in the divine strategy, as exposed in Figure 50.a and b.

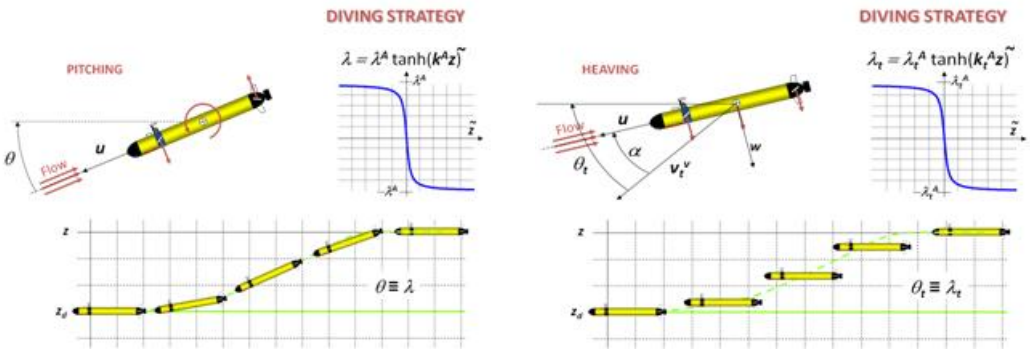

a. diving control in pitching b. diving control in heaving

Figure 50: the different diving strategies

Figure 50.a illustrates the classic diving strategy, used by most of small AUVs such as Gavia or Remus (Figure 51), which do not carry bow control surfaces. Figure 50.b illustrates a second diving strategy that requires an added actuation, in terms of bow diving planes, or explicit buoyancy control (ballast).

a. the Remus AUV © Hydroid b. the Gavia AUV © Hafmynd

Figure 51: existing commercial AUVs

Both the commercial AUVs Remus and Gavia, displayed in Figure 51, are very nice machines, but the lack of bow control surfaces do not allow them to perform a dive simultaneously controlling the heave and pitch dynamics around desired values, while guaranteeing a permanent positive buoyancy. Indeed, the active buoyancy control allows fusing both the diving strategies exposed in Figure 50, but implies the AUV to be negatively buoyant, that makes loose a simple security condition such as the constant positive buoyancy that warrants the machine with the guaranty to reach the surface in the absence of actuation and terrain obstruction.

Another important topic on AUV control is the robustness of the control. Indeed, hydrodynamics modeling, in order to acquire the dynamic model of the vehicle, yields to expected approximations that decrease the control performances.

We have investigated these points during the Meditate Project, and proposed some new solutions, briefly explained in the sequel, and published in the papers referenced at section F.

A. Notation

Before exposing our main results, a necessary preliminary consists in defining the variables and frame we will use in the sequel.

- Let {U} denote the universal earth fixed frame with unit vectors **x** pointing north, **y** pointing east , and **z** pointing down.

- Let {B} denote the body-fixed frame, attached to the metacenter of the vehicle, with unit vectors $\mathbf{x_B}$ pointing to the nose of the vehicle, **y** pointing starboard , and **z** pointing down.
- Let $\{\phi,\theta,\psi\}$ denote the yaw, pitch and roll angles, respectively.
- Let $\{u,v,w\}$ denote the surge, sway and heave velocities, expressed in the {B} frame.
- Let $\{p,q,r\}$ denote the yaw, pitch and roll angular velocities.
- Let denote the total system velocity, expressed in the {B} frame.
- Let a denote the angle of attack (angle between ***u*** and).
- Let q_t denote the absolute vertical orientation of the total velocity (angle between and the horizontal plane

These definitions are illustrated in Figure 52.

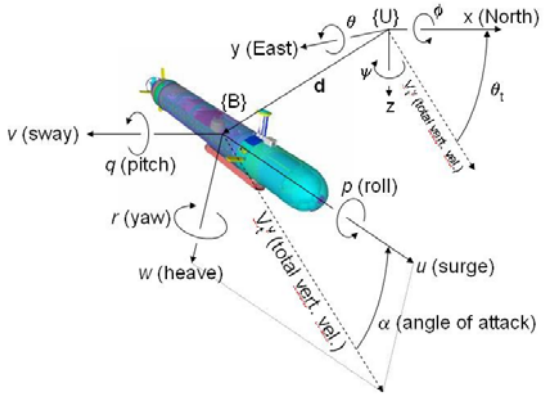

Figure 52: frame definition and problem pose.

B. A full actuation diving strategy for the AUV Taipan 2

We propose a solution that combines both the diving strategies exposed in Figure 50. The control design is based on the non linear Lyapunov approach. It briefly consists in building a positive error function V_1, that fuses both the requirements of controlling the heave and pitch dynamics, in order to follow a desired guidance reference. The guidance functions are named λ and λ_t. Their expressions are exposed in equation 1:

$$\begin{cases} \lambda_t = \lambda_t^A \cdot \tanh(k_t^A \cdot \tilde{z}) \\ \lambda = \lambda^A \cdot \tanh(k^A \cdot \tilde{z})' \end{cases} \quad (1)$$

where $\tilde{z} = z -$ denotes the depth error, with the desired depth, and are the asymptotic approach (i.e maximum pitch and total velocity angles), and and are arbitrary positive gains. Then the control objective is to drive the pitch angle to track (θ) while the angle of the total velocity tracks (θ_t -), and $V_1 = \frac{1}{2} \cdot (\theta \quad \rightarrow \lambda \ )^2 + \frac{1}{2} \cdot (\theta_t \rightarrow$. Note that if λ^A , then the vehicle should dive with a null pitch angle.

Considering a perfect knowledge of the system dynamic parameters, we end up with the solution exposed in [3], where the main results are displayed in Figure 53.

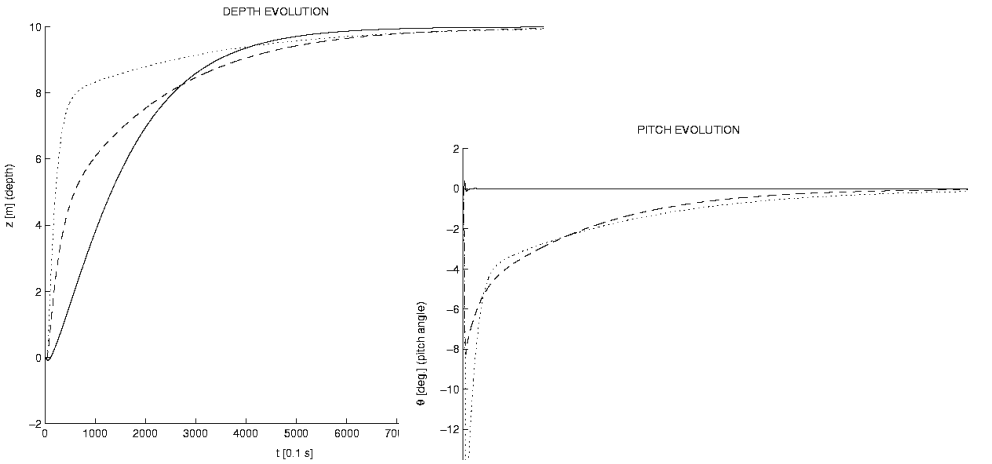

Parameter values of the dynamic control simulation					
$k_\theta = 1$	$k_q = 1$	$k_w = 1$	$k^A = 0.1$	$k_t^A = 0.1$	$z_d = 10m.$
solid line		dashed line		dotted line	
$\lambda^A = 0.0(deg.)$		$\lambda^A = -10.0(deg.)$		$\lambda^A = -20.0(deg.)$	
$\lambda_t^A = -2.0(deg.)$		$\lambda_t^A = -2.0(deg.)$		$\lambda_t^A = -2.0(deg.)$	

Figure 53: nonlinear diving control results

C. Robust diving control for the AUV Taipan 2.

A perfect knowledge of the dynamic parameters of the system is a heavy approximation, which never can be met. Indeed, if we consider the 4 sets of estimated dynamic parameters, randomly computed around the nominal values (Figure 54.a), the previous control exhibits the poor performances illustrated in Figure 54.b.

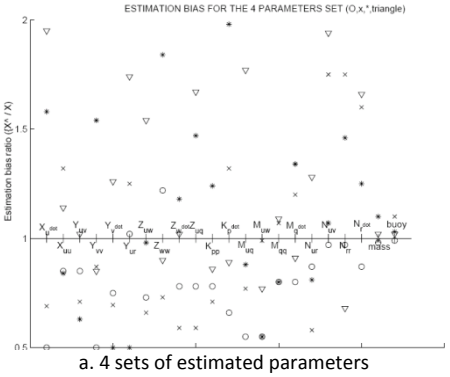

a. 4 sets of estimated parameters

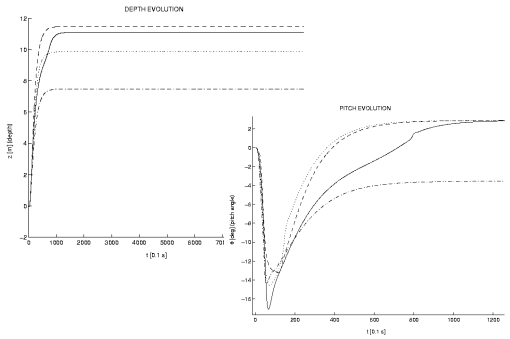

b. undesired effects of the parameters misestimation

Figure 54: parameters misestimation effects

The compensation of these misestimation effects is done in developing an adaptive scheme that allows for the parameters considered in the control expression to evolve according to the minimization of the error function V_1. We end up with the results exposed in Figure 55.a, while the parameters evolution is displayed in Figure 55.b.

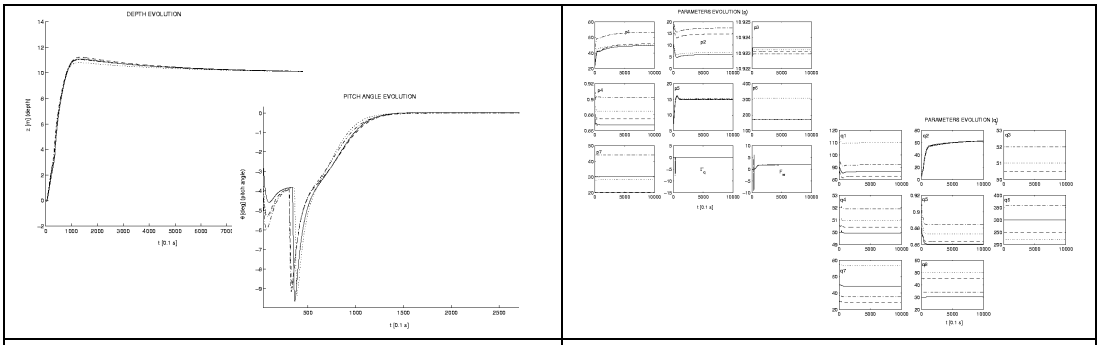

a. Adaptive control results	b. parameters evolution

Figure 55 : adaptive control results

The problem of this method is that nothing can prevent the evolution of the parameters to be bounded, as displayed in figure 56, where the reference is now variable and sensor noise has been added.

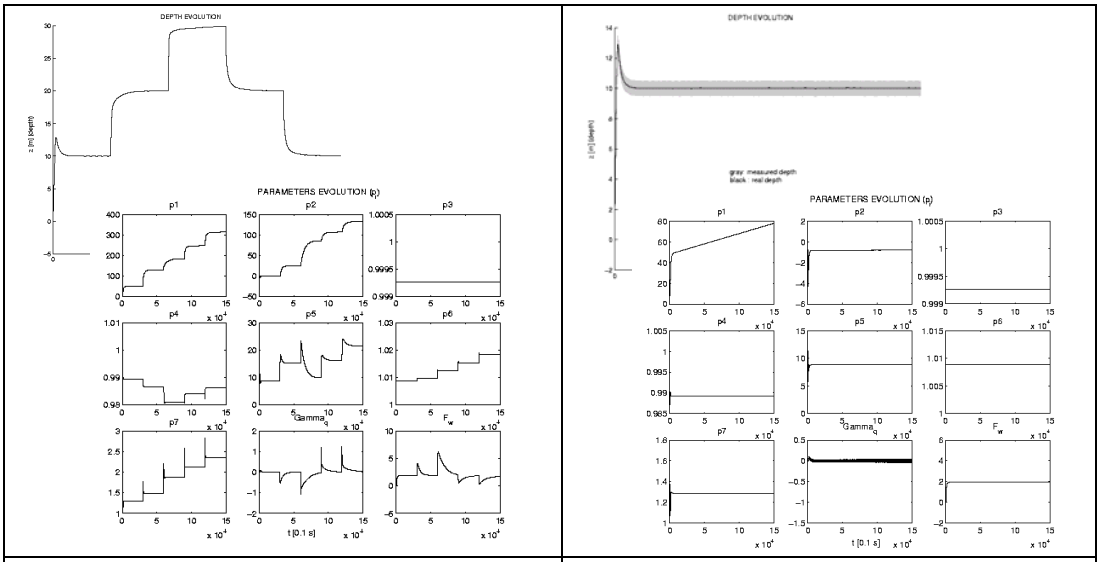

a. varying reference	b. presence of sensor noise

Figure 56 : unbounded evolution of the parameters

To cope with this problem, we proposed another solution based on the development of the switching robust scheme, exposed in [5]. We end up with the results displayed in Figure 57.a, while the evolution of the parameters is displayed in Figure 57.b.

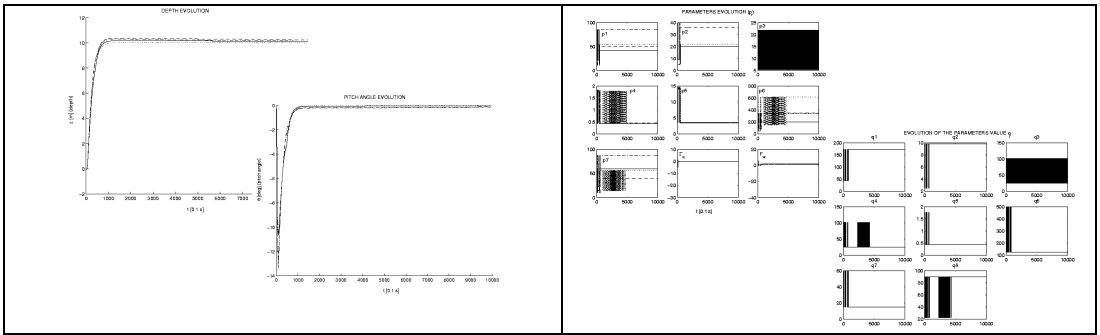

a. switching robust control results	b. switching evolution of the parameters

Figure 56 : Results of the robust switching control

The details of the design of this solution can be find in [6]. This solution has been tested in simulation, and we are currently implementing it on our vehicles.

D. Robust horizontal control of the Taipan 2 AUV.

With the same idea, we have developed a robust horizontal controller for the Taipan 2 and Taipan 300 AUVs. The results are reported in [1] and [7].

E. Robust Control based on High Order Sliding Mode Control

For practical reason, and facility of implementation, we have also investigated the implementation of a robust control based on the principle of Sliding mode controller, extended to higher modes. These results are reported in [8], and [9].

F. References

[1] Lapierre L., Soetanto D., '*Nonlinear Path Following Control of an AUV*', Accepted for publication to the Elsevier Journal of the Oceanic Engineering, November 2006.
URL: http://www.lirmm.fr/~lapierre/Documents/PAPERS/Journaux/ElseVier_JOE/AUVpf.pdf

[2] Lapierre L., '*Underwater Robots Part I: current systems and problem pose*', published in 'Mobile Robotics – Towards New Applications', Edited by Pro Verlag & Advanced Robotic Systems International (ARS), ISBN: 978-3-86611-314-5, November 2006.
URL: http://www.lirmm.fr/~lapierre/Documents/PAPERS/Chapitres_Bouguins/Derniere_Version/17_Lapierre_01_final_060721.pdf

[3] Lapierre L., '*Underwater Robots Part II: existing solutions and open issues*', published in 'Mobile Robotics – Towards New Applications' Edited by Pro Verlag & Advanced Robotic Systems International (ARS), ISBN: 978-3-86611-314-5, November 2006.
URL: http://www.lirmm.fr/~lapierre/Documents/PAPERS/Chapitres_Bouguins/Derniere_Version/18_Lapierre_02_final_060721.pdf

[4] Lapierre L., '*Underwater Robots Part II: existing solutions and open issues*', published in 'Mobile Robotics – Towards New Applications' Edited by Pro Verlag & Advanced Robotic Systems International (ARS), ISBN: 978-3-86611-314-5, November 2006.
URL: http://www.lirmm.fr/~lapierre/Documents/PAPERS/Chapitres_Bouguins/Derniere_Version/18_Lapierre_02_final_060721.pdf

[5] L. Lapierre, V. Creuze and B. Jouvencel, '*Robust Diving Control of an AUV*', MCMC'06, Lisbon, Portugal, 2006.
URL: http://www.lirmm.fr/~lapierre/Documents/PAPERS/Conferences/MCMC2006/LapierreMCMC06.pdf

[6] Lapierre L., Jouvencel B., '*Robust Diving Control of an AUV*', Submitted to the Elsevier Journal of the Oceanic Engineering, March 2006.

[7] Lapierre L., Soetanto D., '*Robust Nonlinear Path Following Control of an AUV*', Submitted to the IEEE Journal of the Oceanic Engineering Society, January 2006.

[8] J.M. Spiewak, B. Jouvencel and P. Fraisse, '*A New Design of AUV for Shallow Water Applications: H160*', in Proceeding of the International Offshore and Polar Engineering Conference, ISOPE'06.

[9] T. Salgado-JimenezJ, J. M. Spiewak, P. Fraisse and B. Jouvencel, '*A Robust Control Algorithm for AUV: Based on a High Order Sliding Mode*', in Proceeding of OCEANS'04, pp. 276-281.